# Observation of $B_s^0 \to \bar{D}^{*0}\phi$ and search for $B^0 \to \bar{D}^0\phi$ decays

R. Aaij *et al.*[*]
(LHCb Collaboration)

(Received 6 July 2018; published 30 October 2018)

The first observation of the $B_s^0 \to \bar{D}^{*0}\phi$ decay is reported, with a significance of more than seven standard deviations, from an analysis of $pp$ collision data corresponding to an integrated luminosity of 3 fb$^{-1}$, collected with the LHCb detector at center-of-mass energies of 7 and 8 TeV. The branching fraction is measured relative to that of the topologically similar decay $B^0 \to \bar{D}^0\pi^+\pi^-$ and is found to be $\mathcal{B}(B_s^0 \to \bar{D}^{*0}\phi) = (3.7 \pm 0.5 \pm 0.3 \pm 0.2) \times 10^{-5}$, where the first uncertainty is statistical, the second systematic, and the third from the branching fraction of the $B^0 \to \bar{D}^0\pi^+\pi^-$ decay. The fraction of longitudinal polarization in this decay is measured to be $f_{\rm L} = (73 \pm 15 \pm 4)\%$. The most precise determination of the branching fraction for the $B_s^0 \to \bar{D}^0\phi$ decay is also obtained, $\mathcal{B}(B_s^0 \to \bar{D}^0\phi) = (3.0 \pm 0.3 \pm 0.2 \pm 0.2) \times 10^{-5}$. An upper limit, $\mathcal{B}(B^0 \to \bar{D}^0\phi) < 2.0\ (2.3) \times 10^{-6}$ at 90% (95%) confidence level is set. A constraint on the $\omega - \phi$ mixing angle $\delta$ is set at $|\delta| < 5.2°$ (5.5°) at 90% (95%) confidence level.

DOI: 10.1103/PhysRevD.98.071103

The precise measurement of the angle $\gamma$ of the Cabibbo-Kobayashi-Maskawa (CKM) Unitarity Triangle [1,2] is a central topic in flavor physics experiments. Its determination at the subdegree level in tree-level open-charm $b$-hadron decays is theoretically clean [3,4] and provides a standard candle for measurements sensitive to new physics effects [5]. In addition to the results from the $B$ factories [6], various measurements from LHCb [7–9] allow the angle $\gamma$ to be determined with an uncertainty of around 5°. However, no single measurement dominates the world average, as the most accurate measurements have an accuracy of $\mathcal{O}(10° - 20°)$ [10,11]. Alternative methods are therefore important to improve the precision. Among them, an analysis of the decays $B_s^0 \to \bar{D}^{(*)0}\phi$ open possibilities to offer competitive experimental precision on the angle $\gamma$ [12–15], where the $\bar{D}^{*0}$ meson can be partially reconstructed [16].

The tree-level Feynman diagrams for the $B_s^0 \to \bar{D}^{(*)0}\phi$ decays are shown in Fig. 1(a). The inclusion of charge-conjugated processes is implied throughout the paper. The decay $B_s^0 \to \bar{D}^0\phi$ was first observed by the LHCb collaboration [17] using a data sample corresponding to an integrated luminosity of 1 fb$^{-1}$, while no prior results exist for $B_s^0 \to \bar{D}^{*0}\phi$ decays. The branching fraction $\mathcal{B}(B_s^0 \to \bar{D}^0\phi)$ is $(3.0 \pm 0.8) \times 10^{-5}$ [17,18]. The $B_s^0 \to \bar{D}^{*0}\phi$ decay is a vector-vector mode and can proceed through different polarization amplitudes. A measurement of its fraction of longitudinal polarization ($f_{\rm L}$) is of particular interest because a significant deviation from unity would confirm previous results from similar color-suppressed $B^0$ decays [19,20], as expected from theory [21,22]. This also helps to constrain QCD models and to search for effects of physics beyond the Standard Model (see review of polarization in $B$ decays in Ref. [18]).

The $B^0 \to \bar{D}^0\phi$ decay can proceed by leading-order Feynman diagrams shown either in Fig. 1(b) or in Fig. 1(c), followed by $\omega - \phi$ mixing. The $W$-exchange decay is suppressed by the Okubo-Zweig-Iizuka (OZI) rule [23–25]. Assuming that the color-suppressed $B^0 \to \bar{D}^0\omega$ decay dominates, the branching fraction of $B^0 \to \bar{D}^0\phi$ is predicted and can be used to determine the mixing angle $\delta$ [26]. The relation between the branching fractions and mixing angle can be written as $\tan^2\delta = \mathcal{B}(B^0 \to \bar{D}^0\phi)/\mathcal{B}(B^0 \to \bar{D}^0\omega) \times \Phi(\omega)/\Phi(\phi)$, where $\Phi(\omega)$ and $\Phi(\phi)$ are the integrals of the phase-space factors computed over the resonant line shapes. A calculation, using a recent result on $\mathcal{B}(B^0 \to \bar{D}^0\omega)$ [19] and taking into account phase-space factors, gives $\mathcal{B}(B^0 \to \bar{D}^0\phi) = (1.6 \pm 0.1) \times 10^{-6}$. The ratio $\Phi(\omega)/\Phi(\phi) = 1.05 \pm 0.01$ is used, where the uncertainty comes from the limited knowledge regarding the shape parameters of the two resonances. The previous experimental upper limit on this branching fraction was $\mathcal{B}(B^0 \to \bar{D}^0\phi) < 11.7 \times 10^{-6}$ at 90% confidence level (C.L.) [27]. The new measurement presented in this paper also allows the $\omega - \phi$ mixing angle to be determined [26,28].

In this paper, results on the $B_{(s)}^0 \to \bar{D}^{(*)0}\phi$ decays are presented, where the $\phi$ meson is reconstructed through its

[*]Full author list given at the end of the article.



 

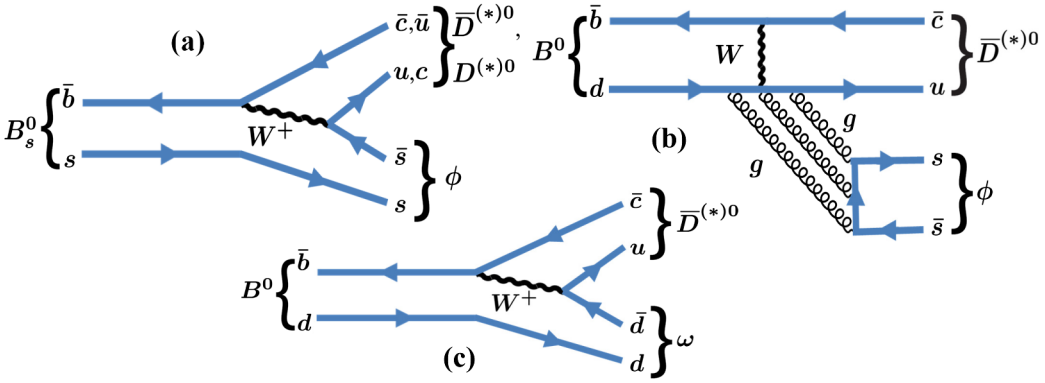


FIG. 1. Diagrams that contribute to the (a) color-suppressed $B_s^0 \to \bar{D}^{(*)0}/D^{(*)0}\phi$, (b) $W$-exchange OZI-suppressed $B^0 \to \bar{D}^0/D^0\phi$ and the (c) color-suppressed $B^0 \to \bar{D}^0\omega$ decays.

decay to a $K^+K^-$ pair and the $\bar{D}^0$ meson decays to $K^+\pi^-$. The $B_s^0 \to \bar{D}^{*0}\phi$ decay is partially reconstructed without inclusion of the neutral pion or photon from the $\bar{D}^{*0}$ meson decay. The analysis is based on a data sample corresponding to 3.0 fb$^{-1}$ of integrated luminosity, of which approximately one third (two thirds) were collected by the LHCb detector from $pp$ collisions at a center-of-mass energy of 7 (8) TeV.

The LHCb detector is a single-arm forward spectrometer covering the pseudorapidity range $2 < \eta < 5$, described in detail in Refs. [29,30]. The online event selection is performed by a trigger [31], which consists of a hardware stage, based on information from the calorimeter and muon systems, followed by a software stage, which applies a full event reconstruction and requires a two-, three- or four-track secondary vertex with a large sum of the component of the momentum transverse to the beam, $p_{\mathrm{T}}$, of the tracks and a significant displacement from all primary $pp$-interaction vertices (PV).

The selection requirements for the $B^0_{(s)} \to \bar{D}^{(*)0}\phi$ signals are the same as those used for the branching fraction measurements of $B^0_{(s)} \to \bar{D}^0K^+K^-$, as described in detail in Ref. [32]. The selection criteria are optimized using the $B^0 \to \bar{D}^0\pi^+\pi^-$ decay as a normalization channel. Signal $B^0_{(s)} \to \bar{D}^0K^+K^-$ candidates are formed by combining $\bar{D}^0$ candidates, reconstructed in the final states $K^+\pi^-$, with two additional particles of opposite charge, identified as kaons, whose tracks are required to be inconsistent with originating from a PV. They must have sufficiently high $p$ and $p_{\mathrm{T}}$ and be within the fiducial acceptance of the two ring-imaging Cherenkov detectors [33] used for particle identification (PID) of charged hadrons. The $\bar{D}^0$ decay products are required to form a good quality vertex with an invariant mass within 25 MeV/$c^2$ of the known $\bar{D}^0$ mass [18]. The $\bar{D}^0$ and two kaon candidates must form a good vertex. The reconstructed $\bar{D}^0$ and $B$ vertices are required to be significantly displaced from any PV. To improve the $B$-candidate invariant-mass resolution, a kinematic fit [34] is used, constraining the $\bar{D}^0$ candidate invariant mass to its known value [18] and the $B$ momentum to point back to the PV with smallest $\chi^2_{\mathrm{IP}}$, where $\chi^2_{\mathrm{IP}}$ is defined as the difference in the vertex-fit $\chi^2$ of a given PV reconstructed with and without the particle under consideration. By requiring the reconstructed $\bar{D}^0$ vertex to be displaced downstream from the reconstructed $B^0$ vertex, backgrounds from both charmless $B$ decays and charmed mesons produced at the PV are reduced to a negligible level. Background from $B^0 \to D^*(2010)^-K^+$ decays is removed by requiring the reconstructed mass difference $m_{\bar{D}^0\pi^-} - m_{\bar{D}^0}$ not to be within $\pm 4.8$ MeV/$c^2$ of its known value [18] after assigning the pion mass to the kaon. To further distinguish signal from combinatorial background, a multivariate analysis based on a Fisher discriminant [35] is applied. The discriminant is optimized by maximizing the statistical significance of $B^0 \to \bar{D}^0\pi^+\pi^-$ candidates selected in a similar way. The discriminant uses the following information: the smallest values of $\chi^2_{\mathrm{IP}}$ and $p_{\mathrm{T}}$ of the prompt tracks from the $B$-decay vertex; the $B$ flight-distance significance; the $D\chi^2_{\mathrm{IP}}$, and the signed minimum cosine of the angle between the direction of one of the prompt tracks from the $B$ decay and the $\bar{D}^0$ meson, as projected in the plane perpendicular to the beam axis.

Candidate $B^0_{(s)} \to \bar{D}^0K^+K^-$ decays with invariant masses in the range $[5000, 6000]$ MeV/$c^2$ are retained. After all selection requirements are applied, less than 1% of the events contain multiple candidates, and a single candidate is chosen based on the fit quality of the $B$- and $D$-meson vertices and on the PID information of the $\bar{D}^0$ decay products. The effect due to the multiple candidate selection is negligible [36].

The distribution of the invariant mass of the $K^+K^-$ pair, $m_{K^+K^-}$, shown in Fig. 2, is obtained from a narrow window, $[2m_K, 2m_K + 90\ \mathrm{MeV}/c^2]$, covering the $\phi$ meson mass [18] and where $m_K$ is the known kaon mass. An extended unbinned maximum-likelihood fit to the invariant-mass distribution of the $\phi$ candidates, $m_{K^+K^-}$, is performed to statistically separate $\phi$ signal from background by means of

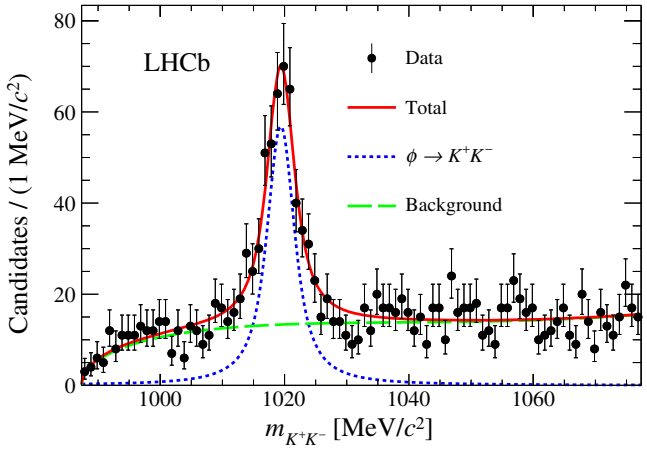


FIG. 2. Fit to the $m_{K^+K^-}$ invariant-mass distribution. Data points are shown in black, the fitted total PDF as a solid (red) line and the component PDFs as dashed lines: (green) background and (blue) signal.

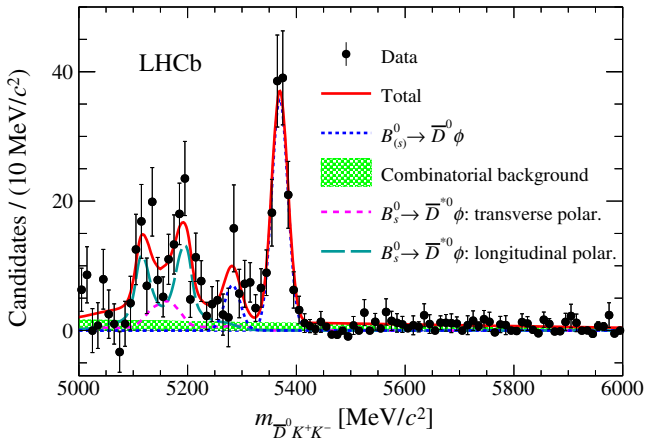


FIG. 3. Fit to the $m_{\bar{D}^0K^+K^-}$ invariant-mass distribution of $\bar{D}^0\phi$ candidates obtained using the *sPlot* technique. Data are shown as black points. The total fit function is displayed as a red solid line and the different contributions are represented as dashed lines and shadowed area: (blue short dashed) the $B_s^0 \to \bar{D}^0\phi$ and $B^0 \to \bar{D}^0\phi$ signal decays, the $B_s^0 \to \bar{D}^{*0}\phi$ signal decay, with (cyan long dashed) longitudinal and (pink middle dashed) transverse polarization and (green shaded area) the combinatorial background.

the *sPlot* technique [37,38]. The $\phi$ meson invariant-mass distribution is modeled with a Breit-Wigner probability density function (PDF) convolved with a Gaussian resolution function. The width of the Breit-Wigner function is fixed to the known $\phi$ width [18]. The PDF for the background is a phase space factor $p \times q$ multiplied by a quadratic function $[1 + ax + b(2x^2 - 1)]$, where $p$ and $q$ are the momentum of the kaon in the $K^+K^-$ rest frame and the momentum of the $\bar{D}^0$ in the $\bar{D}^0K^+K^-$ rest frame, respectively. The variable $x$ is defined as $2 \times (m_{K^+K^-} - 2m_K)/\Delta - 1$, where $\Delta$ is the width of the $m_{K^+K^-}$ mass window so that $x$ is in the range $[-1, 1]$. The parameters $a$ and $b$ are free to vary in the fit. The fit describes the data well ($\chi^2/\mathrm{ndf} = 61/82$). The yields determined by the fit are $427 \pm 30$ for the $\phi \to K^+K^-$ decay and $1152 \pm 41$ for the background.

Figure 3 displays the *sPlot*-projected invariant-mass distribution of $\bar{D}^0K^+K^-$, $m_{\bar{D}^0K^+K^-}$, of $B^0_{(s)} \to \bar{D}^{(*)0}\phi$ candidates. The $m_{K^+K^-}$ invariant mass is used as the discriminating variable and it is only weakly correlated with the $m_{\bar{D}^0K^+K^-}$ invariant mass (less than 6%). A $B_s^0 \to \bar{D}^0\phi$ signal peak is visible at the $B_s^0$ mass, while there is a statistically insignificant excess of $B^0 \to \bar{D}^0\phi$ candidates at the $B^0$ mass. In the region below $m_{B_s^0} - m_{\pi^0}$ (up to resolution effects), a wider structure is visible and can be attributed to the vector-vector decay $B_s^0 \to \bar{D}^{*0}[\to \bar{D}^0\pi^0/\bar{D}^0\gamma]\phi$.

An extended unbinned maximum-likelihood fit is performed to determine the number of $B^0$ and $B_s^0$ decaying into the $\bar{D}^0\phi$ final state and that of the mode $B_s^0 \to \bar{D}^{*0}\phi$ together with the value of the longitudinal polarization fraction $f_\mathrm{L}$. The $B_s^0 \to \bar{D}^0\phi$ mode is modeled by a Gaussian function, for which the mean value and resolution are free parameters. The $B^0$ signal is modeled by a Gaussian function with the same resolution as the $B_s^0$ mode and a mean constrained with respect to that of the $B_s^0$ signal using the known $m_{B_s^0} - m_{B^0}$ mass difference [18]. The $B_s^0 \to \bar{D}^{*0}\phi$ signal is modeled by nonparametric PDFs, built from large simulated samples, using a kernel estimation technique [39]. Its shape, as a function of the $\bar{D}^0K^+K^-$ invariant-mass distribution, strongly depends on the polarization of the decay amplitude. Two extreme polarization configurations are considered: fully longitudinal ($f_\mathrm{L} = 1$) or transverse ($f_\mathrm{L} = 0$). A global PDF for each polarization ($\mathcal{P}_{\mathrm{long/trans}}$) is obtained as the average of the PDF of the two decays $\bar{D}^{*0} \to \bar{D}^0\pi^0/\bar{D}^0\gamma$, weighted according to their relative branching fraction [18]. The total PDF for the $\bar{D}^{*0}\phi$ signal is then modeled as the sum $f_\mathrm{L} \times \mathcal{P}_\mathrm{long} + (1 - f_\mathrm{L}) \times \mathcal{P}_\mathrm{trans}$. The residual background is accounted for with a first-order polynomial function. The yields obtained from this fit are $N_{B_s^0 \to \bar{D}^0\phi} = 132 \pm 13$, $N_{B^0 \to \bar{D}^0\phi} = 26 \pm 11$, and $N_{B_s^0 \to \bar{D}^{*0}\phi} = 163 \pm 19$, with $f_\mathrm{L} = (73 \pm 15)\%$.

The branching fractions of $B^0_{(s)} \to \bar{D}^{(*)0}\phi$ are measured as

$$\frac{\mathcal{B}(B^0_{(s)} \to \bar{D}^{(*)0}\phi)}{\mathcal{B}(B^0 \to \bar{D}^0\pi^+\pi^-)} = \frac{N_{B^0_{(s)} \to \bar{D}^{(*)0}\phi} \times \epsilon(B^0 \to \bar{D}^0\pi^+\pi^-)}{N_{B^0 \to \bar{D}^0\pi^+\pi^-} \times \epsilon(B^0_{(s)} \to \bar{D}^{(*)0}\phi)} \times \frac{\mathcal{F}}{\mathcal{B}(\phi \to K^+K^-)}, \quad (1)$$

where $\mathcal{F}$ is 1 for $B^0$ decays and $f_d/f_s$ for $B_s^0$ decays. In this ratio, the ratio between the signal and normalization modes is required. The efficiency and the number of selected signals for the normalization mode are: $\epsilon(B^0 \to \bar{D}^0\pi^+\pi^-) = (10.6 \pm 0.3) \times 10^{-4}$ and $N_{B^0 \to \bar{D}^0\pi^+\pi^-} = 29\,940 \pm 240$ (see Ref. [32] for details). The efficiency includes various

effects related to reconstruction, triggering and selection of the signal events. Efficiencies are determined from simulation with data-driven corrections applied. The efficiencies of the modes $B_s^0 \to \bar{D}^0\phi$ and $B^0 \to \bar{D}^0\phi$ are statistically consistent and are equal to $\epsilon(B^0_{(s)} \to \bar{D}^0\phi) = (11.1 \pm 0.3) \times 10^{-4}$. For the $B_s^0 \to \bar{D}^{*0}\phi$ decay, the efficiency is obtained as the average of the four following sets of simulated events: fully transverse/longitudinal decays with the decays $\bar{D}^{*0} \to \bar{D}^0\pi^0/\bar{D}^0\gamma$, where the obtained $f_{\rm L} = (73 \pm 15)\%$ and the branching fractions of the $\bar{D}^{*0}$ subdecays are used. The efficiency, after data corrections, is found to be $\epsilon(B_s \to \bar{D}^{*0}\phi) = (10.8 \pm 0.1) \times 10^{-4}$.

In the fit to the $m_{K^+K^-}$ distribution, the background is modeled by a single set of parameters $a$ and $b$. However, the background receives contributions from broad $K^+K^-$ $S$-wave amplitudes, which could be different for the various $B^0_{(s)} \to \bar{D}^{(*)0}K^+K^-$ modes. Since a full amplitude analysis is beyond the scope of this measurement, the following study is performed: the candidates shown in Fig. 2 are divided into three subsamples: $B_s^0 \to \bar{D}^{(*)0}\phi$-like candidates with $m_{\bar{D}^0K^+K^-} \in [5000,5240] \cup [5310,5400]\,{\rm MeV}/c^2$, $B^0 \to \bar{D}^0\phi$-like candidates with $m_{\bar{D}^0K^+K^-} \in [5240, 5310]\ {\rm MeV}/c^2$, and combinatorial background candidates with $m_{\bar{D}^0K^+K^-}$ above 5400 ${\rm MeV}/c^2$. The parameters $a$ and $b$ of the quadratic background function are determined independently for the three subsamples and are found to be consistent with each other. Using the results from the fits to the three subsamples to describe the $K^+K^-$ background, pseudoexperiments are generated to produce $\bar{D}^0K^+K^-$ samples that mimic the data. The signal PDF for the $B^0_{(s)} \to \bar{D}^{(*)0}\phi$ decays and the PDFs for various $b$ -hadron decays are taken from the nominal fit to $m_{\bar{D}^0K^+K^-}$ as described in Ref. [32] are considered. The fits to the $m_{K^+K^-}$ and $m_{\bar{D}^0\phi}$ distributions are then repeated to determine the pull distributions of $N_{B_s^0\to\bar{D}^0\phi}$, $N_{B^0\to\bar{D}^0\phi}$, $N_{B_s^0\to\bar{D}^{*0}\phi}$ and $f_{\rm L}$. The coverage tests perform as expected, except for $N_{B_s^0\to\bar{D}^0\phi}$, for which the data uncertainty is overestimated by about 10%. No correction is applied for this overcoverage. While the fit is unbiased when using a single set of parameters to generate the $K^+K^-$ background, when allowing for different true values of $a$ and $b$ in the different mass regions a bias on the parameter $N_{B^0\to\bar{D}^0\phi}$ is found and corresponds to an overestimation by 7 candidates. This is corrected for the computation of the branching fraction.

Potential sources of systematic uncertainty on the efficiencies are correlated and largely cancel in the quoted ratios of branching fractions. The main differences are related to the PID selection for the $\pi^+\pi^-$ and $K^+K^-$ pairs and to the hardware trigger. For each effect, a systematic uncertainty of 2% is computed, mainly from the PID calibration method and differences between the trigger response in data and simulation [32]. The uncertainty on the known value of $\mathcal{B}(\phi \to K^+K^-)$ is 1% [18]. For the $B_s^0$ modes, an uncertainty of 5.8% related to the fragmentation factor ratio $f_s/f_d$ [40] is accounted for. The yield of the normalization mode is assigned a systematic uncertainty of 2%, where the main contributions are from the modeling of the signal and partially reconstructed background shapes [32].

Sources of systematic uncertainty on the determination of $N_{B^0_{(s)}\to\bar{D}^{(*)0}\phi}$ and $f_{\rm L}$ are related to the fit model of the $m_{K^+K^-}$ distribution and that of the fit to the weighted $\bar{D}^0K^+K^-$ invariant-mass spectrum. The weights from the fits are calculated and the $B^0_{(s)} \to \bar{D}^{(*)0}\phi$ yields and $f_{\rm L}$ are fitted with three different configurations: by varying the natural width of the $\phi$ meson by its uncertainty [18]; by replacing the quadratic part of the $m_{K^+K^-}$ background PDF with a third-order Chebyshev polynomial; and by replacing the $m_{K^+K^-}$ background PDF with an empirical function [41], $\{1 - \exp[-(m - m_0/f)]\} \times (m/m_0)^c + d \times [(m/m_0) - 1]$, where $m_0$ is fixed to $2m_K$ and the parameters $c$, $d$ and $f$ are free to vary in the fit. The largest variations from the nominal model are taken as systematic uncertainties. For the fit to the invariant-mass distribution of the $\bar{D}^0\phi$ candidates, alternative models for $B^0_{(s)} \to \bar{D}^0K^+K^-$ and $B_s^0 \to \bar{D}^{*0}\phi$ are considered: one changing the fit model of the $B^0_{(s)} \to \bar{D}^0\phi$ decays to that used to model $B^0_{(s)} \to \bar{D}^0K^+K^-$, as described in Ref. [32], and others in which the PDFs of the fully transversally/longitudinally polarized $B_s^0 \to \bar{D}^{*0}\phi$ decays are varied within the uncertainties on the ratio of branching fractions $\mathcal{B}(\bar{D}^{*0} \to \bar{D}^0\pi^0)/\mathcal{B}(\bar{D}^{*0} \to \bar{D}^0\gamma)$ [18] and of the efficiencies obtained from simulation. Possible partially reconstructed background from the $B^0 \to \bar{D}^0\phi\pi^+$ and $B_s^0 \to \bar{D}^0\phi\pi^+$ decays are also considered in the fit model. The resulting uncertainties are summed linearly assuming maximal correlation for this kind of systematic uncertainty and correspond to relative values of 4.7%, 31.1%, 5.4% and 4.9% on $N_{B_s^0\to\bar{D}^0\phi}$, $N_{B^0\to\bar{D}^0\phi}$, $N_{B_s^0\to\bar{D}^{*0}\phi}$ and $f_L$, respectively. As the efficiencies depend on the signal decay-time distribution, the effect due to the different lifetimes of the $B_s^0$ eigenstates [42] is considered and found to be 0.8%. When considering the ratio between $\mathcal{B}(B_s^0 \to \bar{D}^{*0}\phi)$ and $\mathcal{B}(B_s^0 \to \bar{D}^0\phi)$ and the longitudinal polarization fraction $f_L$, this systematic uncertainty is doubled to account for unknown strong phases between decay amplitudes and unknown fractions between different angular momenta. See supplemental material [43] for a summary of the various sources of systematic uncertainties.

The ratio of branching fractions $\mathcal{B}(B_s^0 \to \bar{D}^0\phi)/\mathcal{B}(B^0 \to \bar{D}^0\pi^+\pi^-)$ is measured to be $(3.4 \pm 0.4 \pm 0.3)\%$, where the first uncertainty is statistical and the second systematic, and $\mathcal{B}(B_s^0 \to \bar{D}^0\phi)$ to be $(3.0 \pm 0.3 \pm 0.2 \pm 0.2) \times 10^{-5}$, where the third uncertainty is related to the branching fraction of the normalization mode [18,44,45]. The branching fraction is compatible with and more precise than the previous LHCb measurement [17]

and supersedes it. The decay $B_s^0 \to \bar{D}^{*0}\phi$ is observed for the first time, with a significance of more than seven standard deviations estimated using its statistical uncertainty and systematic variations of $N_{B_s^0 \to \bar{D}^{*0}\phi}$. The ratio of branching fractions $\mathcal{B}(B_s^0 \to \bar{D}^{*0}\phi)/\mathcal{B}(B^0 \to \bar{D}^0\pi^+\pi^-)$ is measured to be $(4.2 \pm 0.5 \pm 0.4)\%$ and the branching fraction $\mathcal{B}(B_s^0 \to \bar{D}^{*0}\phi)$ is $(3.7 \pm 0.5 \pm 0.3 \pm 0.2) \times 10^{-5}$. The fraction of longitudinal polarization is measured to be $f_{\rm L} = (73 \pm 15 \pm 4)\%$, which is comparable with measurements from similar color-suppressed $B^0$ decays [19,20]. The ratio of branching fractions $\mathcal{B}(B_s^0 \to \bar{D}^{*0}\phi)/\mathcal{B}(B_s^0 \to \bar{D}^0\phi)$ is $1.23 \pm 0.20 \pm 0.08$.

The ratio of branching fractions of $\mathcal{B}(B^0 \to \bar{D}^0\phi)/\mathcal{B}(B^0 \to \bar{D}^0\pi^+\pi^-)$ is measured to be $(1.2 \pm 0.7 \pm 0.4) \times 10^{-3}$ and the branching fraction $\mathcal{B}(B^0 \to \bar{D}^0\phi)$ to be $(1.1 \pm 0.6 \pm 0.3 \pm 0.1) \times 10^{-6}$. The significance for the $W$-exchange OZI-suppressed decay $B^0 \to \bar{D}^0\phi$ is about two standard deviations. Since there is no significant signal, an upper limit is set as $\mathcal{B}(B^0 \to \bar{D}^0\phi) < 2.0\ (2.3) \times 10^{-6}$ at 90% (95%) C.L., representing a factor of six improvement over the previous limit by the *BABAR* collaboration [27]. The upper limit obtained here is compatible with the updated theoretical prediction $\mathcal{B}(B^0 \to \bar{D}^0\phi) = (1.6 \pm 0.1) \times 10^{-6}$. These results are used to constrain the $\omega - \phi$ mixing angle assuming the dominant contribution to the $B^0 \to \bar{D}^0\phi$ decay is through $\omega - \phi$ mixing. The study in Ref. [28] predicts a mixing angle between 0.45° (at the $\omega$ mass) and 4.65° (at the $\phi$ mass). Using the upper limit in this paper, the constraint $|\delta| < 5.2°(5.5°)$ is set at 90% (95%) C.L. Further studies with more data are therefore motivated.

## ACKNOWLEDGMENTS

We express our gratitude to our colleagues in the CERN accelerator departments for the excellent performance of the LHC. We thank the technical and administrative staff at the LHCb institutes. We acknowledge support from CERN and from the national agencies: CAPES, CNPq, FAPERJ and FINEP (Brazil); MOST and NSFC (China); CNRS/IN2P3 (France); BMBF, DFG and MPG (Germany); INFN (Italy); NWO (Netherlands); MNiSW and NCN (Poland); MEN/IFA (Romania); MinES and FASO (Russia); MinECo (Spain); SNSF and SER (Switzerland); NASU (Ukraine); STFC (United Kingdom); NSF (USA). We acknowledge the computing resources that are provided by CERN, IN2P3 (France), KIT and DESY (Germany), INFN (Italy), SURF (Netherlands), PIC (Spain), GridPP (United Kingdom), RRCKI and Yandex LLC (Russia), CSCS (Switzerland), IFIN-HH (Romania), CBPF (Brazil), PL-GRID (Poland) and OSC (USA). We are indebted to the communities behind the multiple open-source software packages on which we depend. Individual groups or members have received support from AvH Foundation (Germany); EPLANET, Marie Skłodowska-Curie Actions and ERC (European Union); ANR, Labex P2IO and OCEVU, and Région Auvergne-Rhône-Alpes (France); Key Research Program of Frontier Sciences of CAS, CAS PIFI, and the Thousand Talents Program (China); RFBR, RSF and Yandex LLC (Russia); GVA, XuntaGal and GENCAT (Spain); Herchel Smith Fund, the Royal Society, the English-Speaking Union and the Leverhulme Trust (United Kingdom); Laboratory Directed Research and Development program of LANL (USA).

[1] N. Cabibbo, Unitary Symmetry and Leptonic Decays, Phys. Rev. Lett. **10**, 531 (1963).
[2] M. Kobayashi and T. Maskawa, *CP* -violation in the renormalizable theory of weak interaction, Progr. Theor. Phys. **49**, 652 (1973).
[3] J. Brod and J. Zupan, The ultimate theoretical error on $\gamma$ from $B \to DK$ decays, J. High Energy Phys. 01 (2014) 051.
[4] J. Brod, A. Lenz, G. Tetlalmatzi-Xolocotzi, and M. Wiebusch, New physics effects in tree-level decays and the precision in the determination of the quark mixing angle $\gamma$, Phys. Rev. D **92**, 033002 (2015).
[5] J. Charles, S. Descotes-Genon, Z. Ligeti, S. Monteil, M. Papucci, and K. Trabelsi, Future sensitivity to new physics in $B_d$, $B_s$, and K mixings, Phys. Rev. D **89**, 033016 (2014).
[6] A. J. Bevan *et al.* (Belle and *BABAR* Collaborations), The physics of the B factories, Eur. Phys. J. C **74**, 3026 (2014).
[7] Y. Amhis *et al.* (Heavy Flavor Averaging Group), Averages of $b$-hadron, $c$-hadron, and $\tau$-lepton properties as of summer 2016, Eur. Phys. J. C **77**, 895 (2017); updated results and plots available at https://hflav.web.cern.ch.
[8] R. Aaij *et al.* (LHCb Collaboration), Measurement of the CKM angle $\gamma$ from a combination of LHCb results, J. High Energy Phys. 12 (2016) 087.
[9] LHCb Collaboration, Update of the LHCb combination of the CKM angle $\gamma$, Report No. LHCb-CONF-2018-002, 2018.
[10] R. Aaij *et al.* (LHCb Collaboration), Measurement of *CP* asymmetry in $B_s^0 \to D_s^{\mp}K^{\pm}$ decays, J. High Energy Phys. 03 (2018) 059.
[11] R. Aaij *et al.* (LHCb Collaboration), Measurement of the CKM angle $\gamma$ using $B^{\pm} \to DK^{\pm}$ with $D \to K_S^0\pi^+\pi^-$, $K_S^0K^+K^-$ decays, J. High Energy Phys. 08 (2018) 176.
[12] M. Gronau and D. London, How to determine all the angles of the unitarity triangle from $B_d^0 \to DK_S$ and $B_s^0 \to D\phi$, Phys. Lett. B **253**, 483 (1991).
[13] M. Gronau, Y. Grossman, N. Shuhmaher, A. Soffer, and J. Zupan, Using untagged $B^0 \to DK_S$ to determine $\gamma$, Phys. Rev. D **69**, 113003 (2004).

[14] M. Gronau, Y. Grossman, Z. Surujon, and J. Zupan, Enhanced effects on extracting $\gamma$ from untagged $B^0$ and $B_s$ decays, Phys. Lett. B **649**, 61 (2007).

[15] S. Ricciardi, Measuring the CKM angle $\gamma$ at LHCb using untagged $B_s \to D\phi$ decays, Report No. LHCb-PUB-2010-005, 2010.

[16] R. Aaij *et al.* (LHCb Collaboration), Measurement of *CP* observables in $B^\pm \to D^{(*)}K^\pm$ and $B^\pm \to D^{(*)}\pi^\pm$ decays, Phys. Lett. B **777**, 16 (2018).

[17] R. Aaij *et al.* (LHCb Collaboration), Observation of the decay $B_s^0 \to \bar{D}^0\phi$, Phys. Lett. B **727**, 403 (2013).

[18] M. Tanabashi *et al.* (Particle Data Group), Review of particle physics, Phys. Rev. D **98**, 030001 (2018).

[19] J. P. Lees *et al.* (*BABAR* Collaboration), Branching fraction measurements of the color-suppressed decays $\bar{B}^0$ to $D^{(*)0}\pi^0$, $D^{(*)0}\eta$, $D^{(*)0}\omega$, and $D^{(*)0}\eta'$ and measurement of the polarization in the decay $\bar{B}^0 \to D^{*0}\omega$, Phys. Rev. D **84** (2011) 112007; Erratum, Phys. Rev. D **87**, 039901(E) (2013).

[20] D. Matvienko *et al.* (Belle Collaboration), Study of $D^{**}$ production and light hadronic states in the $\bar{B}^0 \to D^{*+}\omega\pi^-$ decay, Phys. Rev. D **92**, 012013 (2015).

[21] A. E. Blechman, S. Mantry, and I. W. Stewart, Heavy quark symmetry in isosinglet non-leptonic B-decays, Phys. Lett. B **608**, 77 (2005).

[22] M. Beneke, J. Rohrer, and D. Yang, Enhanced electroweak penguin amplitude in $B \to VV$ decays, Phys. Rev. Lett. **96**, 141801 (2006).

[23] S. Okubo, $\phi$-meson and unitary symmetry model, Phys. Lett. **5**, 165 (1963).

[24] G. Zweig, An SU(3) model for strong interaction symmetry and its breaking. Version 2, Report No. CERN-TH-412, NP-14146, PRINT-64-170, 22-101, 1964.

[25] J. Iizuka, A systematics and phenomenology of meson family, Prog. Theor. Phys. Suppl. **37**, 21 (1966).

[26] M. Gronau and J. L. Rosner, $B$ decays dominated by $\omega - \phi$ mixing, Phys. Lett. B **666**, 185 (2008).

[27] B. Aubert *et al.* (*BABAR* Collaboration), Search for $B^0 \to \phi(K^+\pi^-)$ decays with large $K^+\pi^-$ invariant mass, Phys. Rev. D **76**, 051103 (2007).

[28] M. Benayoun, P. David, L. DelBuono, O. Leitner, and H. B. O'Connell, The dipion mass spectrum in $e^+e^-$ annihilation and $\tau$ decay: A dynamical ($\rho$, $\omega$, $\phi$) mixing approach, Eur. Phys. J. C **55**, 199 (2008).

[29] A. A. Alves Jr. *et al.* (LHCb Collaboration), The LHCb detector at the LHC, J. Instrum. **3**, S08005 (2008).

[30] R. Aaij *et al.* (LHCb Collaboration), LHCb detector performance, Int. J. Mod. Phys. A **30**, 1530022 (2015).

[31] R. Aaij *et al.*, The LHCb trigger and its performance in 2011, J. Instrum. **8**, P04022 (2013).

[32] R. Aaij *et al.* (LHCb Collaboration), Observation of the decay $B_s^0 \to \bar{D}^0K^+K^-$, arXiv:1807.01891.

[33] M. Adinolfi *et al.*, Performance of the LHCb RICH detector at the LHC, Eur. Phys. J. C **73**, 2431 (2013).

[34] W. D. Hulsbergen, Decay chain fitting with a Kalman filter, Nucl. Instrum. Methods Phys. Res., Sect. A **552**, 566 (2005).

[35] R. A. Fisher, The use of multiple measurements in taxonomic problems, Ann. Eugen. **7**, 179 (1936).

[36] P. Koppenburg, Statistical biases in measurements with multiple candidates, arXiv:1703.01128.

[37] Y. Xie, sFit: A method for background subtraction in maximum likelihood fit, arXiv:0905.0724.

[38] M. Pivk and F. R. Le Diberder, sPlot: A statistical tool to unfold data distributions, Nucl. Instrum. Methods Phys. Res., Sect. A **555**, 356 (2005).

[39] K. S. Cranmer, Kernel estimation in high-energy physics, Comput. Phys. Commun. **136**, 198 (2001).

[40] R. Aaij *et al.* (LHCb Collaboration), Measurement of the fragmentation fraction ratio $f_s/f_d$ and its dependence on $B$ meson kinematics, J. High Energy Phys. 04 (2013) 001; Updated average $f_s/f_d$ $b$-hadron production fraction ratio for 7 TeV $pp$ collisions, Report No. LHCb-CONF-2013-011, 2013.

[41] B. Aubert *et al.* (*BABAR* Collaboration), Evidence for $D^0 - \bar{D}^0$ Mixing, Phys. Rev. Lett. **98**, 211802 (2007).

[42] K. De Bruyn, R. Fleischer, R. Knegjens, P. Koppenburg, M. Merk, and N. Tuning, Branching ratio measurements of $B_s$ decays, Phys. Rev. D **86**, 014027 (2012).

[43] See Supplemental Material at http://link.aps.org/supplemental/10.1103/PhysRevD.98.071103, for the systematic uncertainties from the various sources contributing to the measurements.

[44] A. Kuzmin *et al.* (Belle Collaboration), Study of $\bar{B}^0 \to D^0\pi^+\pi^-$ decays, Phys. Rev. D **76**, 012006 (2007).

[45] R. Aaij *et al.* (LHCb Collaboration), Dalitz plot analysis of $B^0 \to \bar{D}^0\pi^+\pi^-$ decays, Phys. Rev. D **92**, 032002 (2015).



R. Aaij,[27] B. Adeva,[41] M. Adinolfi,[48] C. A. Aidala,[73] Z. Ajaltouni,[5] S. Akar,[59] P. Albicocco,[18] J. Albrecht,[10] F. Alessio,[42] M. Alexander,[53] A. Alfonso Albero,[40] S. Ali,[27] G. Alkhazov,[33] P. Alvarez Cartelle,[55] A. A. Alves Jr,[59] S. Amato,[2] S. Amerio,[23] Y. Amhis,[7] L. An,[3] L. Anderlini,[17] G. Andreassi,[43] M. Andreotti,[16,a] J. E. Andrews,[60] R. B. Appleby,[56] F. Archilli,[27] P. d'Argent,[12] J. Arnau Romeu,[6] A. Artamonov,[39] M. Artuso,[61] K. Arzymatov,[37] E. Aslanides,[6] M. Atzeni,[44] S. Bachmann,[12] J. J. Back,[50] S. Baker,[55] V. Balagura,[7,b] W. Baldini,[16] A. Baranov,[37] R. J. Barlow,[56] S. Barsuk,[7] W. Barter,[56] F. Baryshnikov,[70] V. Batozskaya,[31] B. Batsukh,[61] V. Battista,[43] A. Bay,[43] J. Beddow,[53] F. Bedeschi,[24] I. Bediaga,[1] A. Beiter,[61] L. J. Bel,[27] N. Beliy,[63] V. Bellee,[43] N. Belloli,[20,c] K. Belous,[39] I. Belyaev,[34,42] E. Ben-Haim,[8] G. Bencivenni,[18] S. Benson,[27] S. Beranek,[9] A. Berezhnoy,[35] R. Bernet,[44] D. Berninghoff,[12] E. Bertholet,[8] A. Bertolin,[23] C. Betancourt,[44] F. Betti,[15,42] M. O. Bettler,[49] M. van Beuzekom,[27] Ia. Bezshyiko,[44] S. Bifani,[47] P. Billoir,[8] A. Birnkraut,[10] A. Bizzeti,[17,d] M. Bjørn,[57] T. Blake,[50] F. Blanc,[43] S. Blusk,[61] D. Bobulska,[53] V. Bocci,[26] O. Boente Garcia,[41] T. Boettcher,[58] A. Bondar,[38,e]

N. Bondar,[33] S. Borghi,[56,42] M. Borisyak,[37] M. Borsato,[41,42] F. Bossu,[7] M. Boubdir,[9] T. J. V. Bowcock,[54] C. Bozzi,[16,42] S. Braun,[12] M. Brodski,[42] J. Brodzicka,[29] D. Brundu,[22] E. Buchanan,[48] A. Buonaura,[44] C. Burr,[56] A. Bursche,[22] J. Buytaert,[42] W. Byczynski,[42] S. Cadeddu,[22] H. Cai,[64] R. Calabrese,[16,a] R. Calladine,[47] M. Calvi,[20,c] M. Calvo Gomez,[40,f] A. Camboni,[40,f] P. Campana,[18] D. H. Campora Perez,[42] L. Capriotti,[56] A. Carbone,[15,g] G. Carboni,[25] R. Cardinale,[19,h] A. Cardini,[22] P. Carniti,[20,c] L. Carson,[52] K. Carvalho Akiba,[2] G. Casse,[54] L. Cassina,[20] M. Cattaneo,[42] G. Cavallero,[19,h] R. Cenci,[24,i] D. Chamont,[7] M. G. Chapman,[48] M. Charles,[8] Ph. Charpentier,[42] G. Chatzikonstantinidis,[47] M. Chefdeville,[4] V. Chekalina,[37] C. Chen,[3] S. Chen,[22] S.-G. Chitic,[42] V. Chobanova,[41] M. Chrzaszcz,[42] A. Chubykin,[33] P. Ciambrone,[18] X. Cid Vidal,[41] G. Ciezarek,[42] P. E. L. Clarke,[52] M. Clemencic,[42] H. V. Cliff,[49] J. Closier,[42] V. Coco,[42] J. Cogan,[6] E. Cogneras,[5] L. Cojocariu,[32] P. Collins,[42] T. Colombo,[42] A. Comerma-Montells,[12] A. Contu,[22] G. Coombs,[42] S. Coquereau,[40] G. Corti,[42] M. Corvo,[16,a] C. M. Costa Sobral,[50] B. Couturier,[42] G. A. Cowan,[52] D. C. Craik,[58] A. Crocombe,[50] M. Cruz Torres,[1] R. Currie,[52] C. D'Ambrosio,[42] F. Da Cunha Marinho,[2] C. L. Da Silva,[74] E. Dall'Occo,[27] J. Dalseno,[48] A. Danilina,[34] A. Davis,[3] O. De Aguiar Francisco,[42] K. De Bruyn,[42] S. De Capua,[56] M. De Cian,[43] J. M. De Miranda,[1] L. De Paula,[2] M. De Serio,[14,j] P. De Simone,[18] C. T. Dean,[53] D. Decamp,[4] L. Del Buono,[8] B. Delaney,[49] H.-P. Dembinski,[11] M. Demmer,[10] A. Dendek,[30] D. Derkach,[37] O. Deschamps,[5] F. Dettori,[54] B. Dey,[65] A. Di Canto,[42] P. Di Nezza,[18] S. Didenko,[70] H. Dijkstra,[42] F. Dordei,[42] M. Dorigo,[42,k] A. Dosil Suárez,[41] L. Douglas,[53] A. Dovbnya,[45] K. Dreimanis,[54] L. Dufour,[27] G. Dujany,[8] P. Durante,[42] J. M. Durham,[74] D. Dutta,[56] R. Dzhelyadin,[39] M. Dziewiecki,[12] A. Dziurda,[42] A. Dzyuba,[33] S. Easo,[51] U. Egede,[55] V. Egorychev,[34] S. Eidelman,[38,e] S. Eisenhardt,[52] U. Eitschberger,[10] R. Ekelhof,[10] L. Eklund,[53] S. Ely,[61] A. Ene,[32] S. Escher,[9] S. Esen,[27] H. M. Evans,[49] T. Evans,[57] A. Falabella,[15] N. Farley,[47] S. Farry,[54] D. Fazzini,[20,42,c] L. Federici,[25] G. Fernandez,[40] P. Fernandez Declara,[42] A. Fernandez Prieto,[41] F. Ferrari,[15] L. Ferreira Lopes,[43] F. Ferreira Rodrigues,[2] M. Ferro-Luzzi,[42] S. Filippov,[36] R. A. Fini,[14] M. Fiorini,[16,a] M. Firlej,[30] C. Fitzpatrick,[43] T. Fiutowski,[30] F. Fleuret,[7,b] M. Fontana,[22,42] F. Fontanelli,[19,h] R. Forty,[42] V. Franco Lima,[54] M. Frank,[42] C. Frei,[42] J. Fu,[21,l] W. Funk,[42] C. Färber,[42] M. Féo Pereira Rivello Carvalho,[27] E. Gabriel,[52] A. Gallas Torreira,[41] D. Galli,[15,g] S. Gallorini,[23] S. Gambetta,[52] M. Gandelman,[2] P. Gandini,[21] Y. Gao,[3] L. M. Garcia Martin,[72] B. Garcia Plana,[41] J. García Pardiñas,[44] J. Garra Tico,[49] L. Garrido,[40] D. Gascon,[40] C. Gaspar,[42] L. Gavardi,[10] G. Gazzoni,[5] D. Gerick,[12] E. Gersabeck,[56] M. Gersabeck,[56] T. Gershon,[50] Ph. Ghez,[4] S. Gianì,[43] V. Gibson,[49] O. G. Girard,[43] L. Giubega,[32] K. Gizdov,[52] V. V. Gligorov,[8] D. Golubkov,[34] A. Golutvin,[55,70] A. Gomes,[1,m] I. V. Gorelov,[35] C. Gotti,[20,c] E. Govorkova,[27] J. P. Grabowski,[12] R. Graciani Diaz,[40] L. A. Granado Cardoso,[42] E. Graugés,[40] E. Graverini,[44] G. Graziani,[17] A. Grecu,[32] R. Greim,[27] P. Griffith,[22] L. Grillo,[56] L. Gruber,[42] B. R. Gruberg Cazon,[57] O. Grünberg,[67] C. Gu,[3] E. Gushchin,[36] Yu. Guz,[39,42] T. Gys,[42] C. Göbel,[62] T. Hadavizadeh,[57] C. Hadjivasiliou,[5] G. Haefeli,[43] C. Haen,[42] S. C. Haines,[49] B. Hamilton,[60] X. Han,[12] T. H. Hancock,[57] S. Hansmann-Menzemer,[12] N. Harnew,[57] S. T. Harnew,[48] C. Hasse,[42] M. Hatch,[42] J. He,[63] M. Hecker,[55] K. Heinicke,[10] A. Heister,[9] K. Hennessy,[54] L. Henry,[72] E. van Herwijnen,[42] M. Heß,[67] A. Hicheur,[2] D. Hill,[57] M. Hilton,[56] P. H. Hopchev,[43] W. Hu,[65] W. Huang,[63] Z. C. Huard,[59] W. Hulsbergen,[27] T. Humair,[55] M. Hushchyn,[37] D. Hutchcroft,[54] D. Hynds,[27] P. Ibis,[10] M. Idzik,[30] P. Ilten,[47] K. Ivshin,[33] R. Jacobsson,[42] J. Jalocha,[57] E. Jans,[27] A. Jawahery,[60] F. Jiang,[3] M. John,[57] D. Johnson,[42] C. R. Jones,[49] C. Joram,[42] B. Jost,[42] N. Jurik,[57] S. Kandybei,[45] M. Karacson,[42] J. M. Kariuki,[48] S. Karodia,[53] N. Kazeev,[37] M. Kecke,[12] F. Keizer,[49] M. Kelsey,[61] M. Kenzie,[49] T. Ketel,[28] E. Khairullin,[37] B. Khanji,[12] C. Khurewathanakul,[43] K. E. Kim,[61] T. Kirn,[9] S. Klaver,[18] K. Klimaszewski,[31] T. Klimkovich,[11] S. Koliiev,[46] M. Kolpin,[12] R. Kopecna,[12] P. Koppenburg,[27] S. Kotriakhova,[33] M. Kozeiha,[5] L. Kravchuk,[36] M. Kreps,[50] F. Kress,[55] P. Krokovny,[38,e] W. Krupa,[30] W. Krzemien,[31] W. Kucewicz,[29,n] M. Kucharczyk,[29] V. Kudryavtsev,[38,e] A. K. Kuonen,[43] T. Kvaratskheliya,[34,42] D. Lacarrere,[42] G. Lafferty,[56] A. Lai,[22] D. Lancierini,[44] G. Lanfranchi,[18] C. Langenbruch,[9] T. Latham,[50] C. Lazzeroni,[47] R. Le Gac,[6] A. Leflat,[35] J. Lefrançois,[7] R. Lefèvre,[5] F. Lemaitre,[42] O. Leroy,[6] T. Lesiak,[29] B. Leverington,[12] P.-R. Li,[63] T. Li,[3] Z. Li,[61] X. Liang,[61] T. Likhomanenko,[69] R. Lindner,[42] F. Lionetto,[44] V. Lisovskyi,[7] X. Liu,[3] D. Loh,[50] A. Loi,[22] I. Longstaff,[53] J. H. Lopes,[2] D. Lucchesi,[23,o] M. Lucio Martinez,[41] A. Lupato,[23] E. Luppi,[16,a] O. Lupton,[42] A. Lusiani,[24] X. Lyu,[63] F. Machefert,[7] F. Maciuc,[32] V. Macko,[43] P. Mackowiak,[10] S. Maddrell-Mander,[48] O. Maev,[33,42] K. Maguire,[56] D. Maisuzenko,[33] M. W. Majewski,[30] S. Malde,[57] B. Malecki,[29] A. Malinin,[69] T. Maltsev,[38,e] G. Manca,[22,p] G. Mancinelli,[6] D. Marangotto,[21,l] J. Maratas,[5,q] J. F. Marchand,[4] U. Marconi,[15] C. Marin Benito,[40] M. Marinangeli,[43] P. Marino,[43] J. Marks,[12] G. Martellotti,[26] M. Martin,[6] M. Martinelli,[43] D. Martinez Santos,[41] F. Martinez Vidal,[72] A. Massafferri,[1] R. Matev,[42] A. Mathad,[50] Z. Mathe,[42] C. Matteuzzi,[20] A. Mauri,[44] E. Maurice,[7,b] B. Maurin,[43] A. Mazurov,[47] M. McCann,[55,42] A. McNab,[56] R. McNulty,[13] J. V. Mead,[54] B. Meadows,[59] C. Meaux,[6] F. Meier,[10] N. Meinert,[67] D. Melnychuk,[31] M. Merk,[27] A. Merli,[21,l] E. Michielin,[23]

D. A. Milanes,[66] E. Millard,[50] M.-N. Minard,[4] L. Minzoni,[16,a] D. S. Mitzel,[12] A. Mogini,[8] J. Molina Rodriguez,[1,r] T. Mombächer,[10] I. A. Monroy,[66] S. Monteil,[5] M. Morandin,[23] G. Morello,[18] M. J. Morello,[24,s] O. Morgunova,[69] J. Moron,[30] A. B. Morris,[6] R. Mountain,[61] F. Muheim,[52] M. Mulder,[27] D. Müller,[42] J. Müller,[10] K. Müller,[44] V. Müller,[10] P. Naik,[48] T. Nakada,[43] R. Nandakumar,[51] A. Nandi,[57] T. Nanut,[43] I. Nasteva,[2] M. Needham,[52] N. Neri,[21] S. Neubert,[12] N. Neufeld,[42] M. Neuner,[12] T. D. Nguyen,[43] C. Nguyen-Mau,[43,t] S. Nieswand,[9] R. Niet,[10] N. Nikitin,[35] A. Nogay,[69] D. P. O'Hanlon,[15] A. Oblakowska-Mucha,[30] V. Obraztsov,[39] S. Ogilvy,[18] R. Oldeman,[22,p] C. J. G. Onderwater,[68] A. Ossowska,[29] J. M. Otalora Goicochea,[2] P. Owen,[44] A. Oyanguren,[72] P. R. Pais,[43] A. Palano,[14] M. Palutan,[18,42] G. Panshin,[71] A. Papanestis,[51] M. Pappagallo,[52] L. L. Pappalardo,[16,a] W. Parker,[60] C. Parkes,[56] G. Passaleva,[17,42] A. Pastore,[14] M. Patel,[55] C. Patrignani,[15,g] A. Pearce,[42] A. Pellegrino,[27] G. Penso,[26] M. Pepe Altarelli,[42] S. Perazzini,[42] D. Pereima,[34] P. Perret,[5] L. Pescatore,[43] K. Petridis,[48] A. Petrolini,[19,h] A. Petrov,[69] M. Petruzzo,[21,l] B. Pietrzyk,[4] G. Pietrzyk,[43] M. Pikies,[29] D. Pinci,[26] J. Pinzino,[42] F. Pisani,[42] A. Pistone,[19,h] A. Piucci,[12] V. Placinta,[32] S. Playfer,[52] J. Plews,[47] M. Plo Casasus,[41] F. Polci,[8] M. Poli Lener,[18] A. Poluektov,[50] N. Polukhina,[70,u] I. Polyakov,[61] E. Polycarpo,[2] G. J. Pomery,[48] S. Ponce,[42] A. Popov,[39] D. Popov,[47,11] S. Poslavskii,[39] C. Potterat,[2] E. Price,[48] J. Prisciandaro,[41] C. Prouve,[48] V. Pugatch,[46] A. Puig Navarro,[44] H. Pullen,[57] G. Punzi,[24,i] W. Qian,[63] J. Qin,[63] R. Quagliani,[8] B. Quintana,[5] B. Rachwal,[30] J. H. Rademacker,[48] M. Rama,[24] M. Ramos Pernas,[41] M. S. Rangel,[2] F. Ratnikov,[37,v] G. Raven,[28] M. Ravonel Salzgeber,[42] M. Reboud,[4] F. Redi,[43] S. Reichert,[10] A. C. dos Reis,[1] F. Reiss,[8] C. Remon Alepuz,[72] Z. Ren,[3] V. Renaudin,[7] S. Ricciardi,[51] S. Richards,[48] K. Rinnert,[54] P. Robbe,[7] A. Robert,[8] A. B. Rodrigues,[43] E. Rodrigues,[59] J. A. Rodriguez Lopez,[66] A. Rogozhnikov,[37] S. Roiser,[42] A. Rollings,[57] V. Romanovskiy,[39] A. Romero Vidal,[41] M. Rotondo,[18] M. S. Rudolph,[61] T. Ruf,[42] J. Ruiz Vidal,[72] J. J. Saborido Silva,[41] N. Sagidova,[33] B. Saitta,[22,p] V. Salustino Guimaraes,[62] C. Sanchez Gras,[27] C. Sanchez Mayordomo,[72] B. Sanmartin Sedes,[41] R. Santacesaria,[26] C. Santamarina Rios,[41] M. Santimaria,[18] E. Santovetti,[25,w] G. Sarpis,[56] A. Sarti,[18,x] C. Satriano,[26,y] A. Satta,[25] M. Saur,[63] D. Savrina,[34,35] S. Schael,[9] M. Schellenberg,[10] M. Schiller,[53] H. Schindler,[42] M. Schmelling,[11] T. Schmelzer,[10] B. Schmidt,[42] O. Schneider,[43] A. Schopper,[42] H. F. Schreiner,[59] M. Schubiger,[43] M. H. Schune,[7] R. Schwemmer,[42] B. Sciascia,[18] A. Sciubba,[26,x] A. Semennikov,[34] E. S. Sepulveda,[8] A. Sergi,[47,42] N. Serra,[44] J. Serrano,[6] L. Sestini,[23] P. Seyfert,[42] M. Shapkin,[39] Y. Shcheglov,[33] T. Shears,[54] L. Shekhtman,[38,e] V. Shevchenko,[69] E. Shmanin,[70] B. G. Siddi,[16] R. Silva Coutinho,[44] L. Silva de Oliveira,[2] G. Simi,[23,o] S. Simone,[14,j] N. Skidmore,[12] T. Skwarnicki,[61] E. Smith,[9] I. T. Smith,[52] M. Smith,[55] M. Soares,[15] l. Soares Lavra,[1] M. D. Sokoloff,[59] F. J. P. Soler,[53] B. Souza De Paula,[2] B. Spaan,[10] P. Spradlin,[53] F. Stagni,[42] M. Stahl,[12] S. Stahl,[42] P. Stefko,[43] S. Stefkova,[55] O. Steinkamp,[44] S. Stemmle,[12] O. Stenyakin,[39] M. Stepanova,[33] H. Stevens,[10] S. Stone,[61] B. Storaci,[44] S. Stracka,[24,i] M. E. Stramaglia,[43] M. Straticiuc,[32] U. Straumann,[44] S. Strokov,[71] J. Sun,[3] L. Sun,[64] K. Swientek,[30] V. Syropoulos,[28] T. Szumlak,[30] M. Szymanski,[63] S. T'Jampens,[4] Z. Tang,[3] A. Tayduganov,[6] T. Tekampe,[10] G. Tellarini,[16] F. Teubert,[42] E. Thomas,[42] J. van Tilburg,[27] M. J. Tilley,[55] V. Tisserand,[5] M. Tobin,[43] S. Tolk,[42] L. Tomassetti,[16,a] D. Tonelli,[24] D. Y. Tou,[8] R. Tourinho Jadallah Aoude,[1] E. Tournefier,[4] M. Traill,[53] M. T. Tran,[43] A. Trisovic,[49] A. Tsaregorodtsev,[6] A. Tully,[49] N. Tuning,[27,42] A. Ukleja,[31] A. Usachov,[7] A. Ustyuzhanin,[37] U. Uwer,[12] C. Vacca,[22,p] A. Vagner,[71] V. Vagnoni,[15] A. Valassi,[42] S. Valat,[42] G. Valenti,[15] R. Vazquez Gomez,[42] P. Vazquez Regueiro,[41] S. Vecchi,[16] M. van Veghel,[27] J. J. Velthuis,[48] M. Veltri,[17,z] G. Veneziano,[57] A. Venkateswaran,[61] T. A. Verlage,[9] M. Vernet,[5] M. Vesterinen,[57] J. V. Viana Barbosa,[42] D. Vieira,[63] M. Vieites Diaz,[41] H. Viemann,[67] X. Vilasis-Cardona,[40,f] A. Vitkovskiy,[27] M. Vitti,[49] V. Volkov,[35] A. Vollhardt,[44] B. Voneki,[42] A. Vorobyev,[33] V. Vorobyev,[38,e] C. Voß,[9] J. A. de Vries,[27] C. Vázquez Sierra,[27] R. Waldi,[67] J. Walsh,[24] J. Wang,[61] M. Wang,[3] Y. Wang,[65] Z. Wang,[44] D. R. Ward,[49] H. M. Wark,[54] N. K. Watson,[47] D. Websdale,[55] A. Weiden,[44] C. Weisser,[58] M. Whitehead,[9] J. Wicht,[50] G. Wilkinson,[57] M. Wilkinson,[61] M. R. J. Williams,[56] M. Williams,[58] T. Williams,[47] F. F. Wilson,[51,42] J. Wimberley,[60] M. Winn,[7] J. Wishahi,[10] W. Wislicki,[31] M. Witek,[29] G. Wormser,[7] S. A. Wotton,[49] K. Wyllie,[42] D. Xiao,[65] Y. Xie,[65] A. Xu,[3] M. Xu,[65] Q. Xu,[63] Z. Xu,[3] Z. Xu,[4] Z. Yang,[3] Z. Yang,[60] Y. Yao,[61] H. Yin,[65] J. Yu,[65,aa] X. Yuan,[61] O. Yushchenko,[39] K. A. Zarebski,[47] M. Zavertyaev,[11,u] D. Zhang,[65] L. Zhang,[3] W. C. Zhang,[3,bb] Y. Zhang,[7] A. Zhelezov,[12] Y. Zheng,[63] X. Zhu,[3] V. Zhukov,[9,35] J. B. Zonneveld,[52] and S. Zucchelli[15]

(LHCb Collaboration)

[1]*Centro Brasileiro de Pesquisas Físicas (CBPF), Rio de Janeiro, Brazil*
[2]*Universidade Federal do Rio de Janeiro (UFRJ), Rio de Janeiro, Brazil*
[3]*Center for High Energy Physics, Tsinghua University, Beijing, China*

[4]Université Grenoble Alpes, Université Savoie Mont Blanc, CNRS, IN2P3-LAPP, Annecy, France
[5]Clermont Université, Université Blaise Pascal, CNRS/IN2P3, LPC, Clermont-Ferrand, France
[6]Aix Marseille Université, CNRS/IN2P3, CPPM, Marseille, France
[7]LAL, Université Paris-Sud, CNRS/IN2P3, Université Paris-Saclay, Orsay, France
[8]LPNHE, Sorbonne Université, Paris Diderot Sorbonne Paris Cité, CNRS/IN2P3, Paris, France
[9]I. Physikalisches Institut, RWTH Aachen University, Aachen, Germany
[10]Fakultät Physik, Technische Universität Dortmund, Dortmund, Germany
[11]Max-Planck-Institut für Kernphysik (MPIK), Heidelberg, Germany
[12]Physikalisches Institut, Ruprecht-Karls-Universität Heidelberg, Heidelberg, Germany
[13]School of Physics, University College Dublin, Dublin, Ireland
[14]INFN Sezione di Bari, Bari, Italy
[15]INFN Sezione di Bologna, Bologna, Italy
[16]INFN Sezione di Ferrara, Ferrara, Italy
[17]INFN Sezione di Firenze, Firenze, Italy
[18]INFN Laboratori Nazionali di Frascati, Frascati, Italy
[19]INFN Sezione di Genova, Genova, Italy
[20]INFN Sezione di Milano-Bicocca, Milano, Italy
[21]INFN Sezione di Milano, Milano, Italy
[22]INFN Sezione di Cagliari, Monserrato, Italy
[23]INFN Sezione di Padova, Padova, Italy
[24]INFN Sezione di Pisa, Pisa, Italy
[25]INFN Sezione di Roma Tor Vergata, Roma, Italy
[26]INFN Sezione di Roma La Sapienza, Roma, Italy
[27]Nikhef National Institute for Subatomic Physics, Amsterdam, Netherlands
[28]Nikhef National Institute for Subatomic Physics and VU University Amsterdam, Amsterdam, Netherlands
[29]Henryk Niewodniczanski Institute of Nuclear Physics Polish Academy of Sciences, Kraków, Poland
[30]AGH - University of Science and Technology, Faculty of Physics and Applied Computer Science, Kraków, Poland
[31]National Center for Nuclear Research (NCBJ), Warsaw, Poland
[32]Horia Hulubei National Institute of Physics and Nuclear Engineering, Bucharest-Magurele, Romania
[33]Petersburg Nuclear Physics Institute (PNPI), Gatchina, Russia
[34]Institute of Theoretical and Experimental Physics (ITEP), Moscow, Russia
[35]Institute of Nuclear Physics, Moscow State University (SINP MSU), Moscow, Russia
[36]Institute for Nuclear Research of the Russian Academy of Sciences (INR RAS), Moscow, Russia
[37]Yandex School of Data Analysis, Moscow, Russia
[38]Budker Institute of Nuclear Physics (SB RAS), Novosibirsk, Russia
[39]Institute for High Energy Physics (IHEP), Protvino, Russia
[40]ICCUB, Universitat de Barcelona, Barcelona, Spain
[41]Instituto Galego de Física de Altas Enerxías (IGFAE), Universidade de Santiago de Compostela, Santiago de Compostela, Spain
[42]European Organization for Nuclear Research (CERN), Geneva, Switzerland
[43]Institute of Physics, Ecole Polytechnique Fédérale de Lausanne (EPFL), Lausanne, Switzerland
[44]Physik-Institut, Universität Zürich, Zürich, Switzerland
[45]NSC Kharkiv Institute of Physics and Technology (NSC KIPT), Kharkiv, Ukraine
[46]Institute for Nuclear Research of the National Academy of Sciences (KINR), Kyiv, Ukraine
[47]University of Birmingham, Birmingham, United Kingdom
[48]H.H. Wills Physics Laboratory, University of Bristol, Bristol, United Kingdom
[49]Cavendish Laboratory, University of Cambridge, Cambridge, United Kingdom
[50]Department of Physics, University of Warwick, Coventry, United Kingdom
[51]STFC Rutherford Appleton Laboratory, Didcot, United Kingdom
[52]School of Physics and Astronomy, University of Edinburgh, Edinburgh, United Kingdom
[53]School of Physics and Astronomy, University of Glasgow, Glasgow, United Kingdom
[54]Oliver Lodge Laboratory, University of Liverpool, Liverpool, United Kingdom
[55]Imperial College London, London, United Kingdom
[56]School of Physics and Astronomy, University of Manchester, Manchester, United Kingdom
[57]Department of Physics, University of Oxford, Oxford, United Kingdom
[58]Massachusetts Institute of Technology, Cambridge, Massachusetts, USA
[59]University of Cincinnati, Cincinnati, Ohio, USA
[60]University of Maryland, College Park, Maryland, USA
[61]Syracuse University, Syracuse, New York, USA

[62]*Pontifícia Universidade Católica do Rio de Janeiro (PUC-Rio), Rio de Janeiro, Brazil*
*[associated with Universidade Federal do Rio de Janeiro (UFRJ), Rio de Janeiro, Brazil]*
[63]*University of Chinese Academy of Sciences, Beijing, China*
*(associated with Center for High Energy Physics, Tsinghua University, Beijing, China)*
[64]*School of Physics and Technology, Wuhan University, Wuhan, China*
*(associated with Center for High Energy Physics, Tsinghua University, Beijing, China)*
[65]*Institute of Particle Physics, Central China Normal University, Wuhan, Hubei, China*
*(associated with Center for High Energy Physics, Tsinghua University, Beijing, China)*
[66]*Departamento de Fisica, Universidad Nacional de Colombia, Bogota, Colombia*
*(associated with LPNHE, Sorbonne Université, Paris Diderot Sorbonne Paris Cité, CNRS/IN2P3, Paris, France)*
[67]*Institut für Physik, Universität Rostock, Rostock, Germany*
*(associated with Physikalisches Institut, Ruprecht-Karls-Universität Heidelberg, Heidelberg, Germany)*
[68]*Van Swinderen Institute, University of Groningen, Groningen, Netherlands*
*(associated with Nikhef National Institute for Subatomic Physics, Amsterdam, Netherlands)*
[69]*National Research Centre Kurchatov Institute, Moscow, Russia*
*[associated with Institute of Theoretical and Experimental Physics (ITEP), Moscow, Russia]*
[70]*National University of Science and Technology "MISIS", Moscow, Russia*
*[associated with Institute of Theoretical and Experimental Physics (ITEP), Moscow, Russia]*
[71]*National Research Tomsk Polytechnic University, Tomsk, Russia*
*[associated with Institute of Theoretical and Experimental Physics (ITEP), Moscow, Russia]*
[72]*Instituto de Fisica Corpuscular, Centro Mixto Universidad de Valencia - CSIC, Valencia, Spain*
*(associated with ICCUB, Universitat de Barcelona, Barcelona, Spain)*
[73]*University of Michigan, Ann Arbor, Michigan, USA*
*(associated with Syracuse University, Syracuse, New York, USA)*
[74]*Los Alamos National Laboratory (LANL), Los Alamos, New Mexico, USA*
*(associated with Syracuse University, Syracuse, New York, USA)*

[a]Also at Università di Ferrara, Ferrara, Italy.
[b]Also at Laboratoire Leprince-Ringuet, Palaiseau, France.
[c]Also at Università di Milano Bicocca, Milano, Italy.
[d]Also at Università di Modena e Reggio Emilia, Modena, Italy.
[e]Also at Novosibirsk State University, Novosibirsk, Russia.
[f]Also at LIFAELS, La Salle, Universitat Ramon Llull, Barcelona, Spain.
[g]Also at Università di Bologna, Bologna, Italy.
[h]Also at Università di Genova, Genova, Italy.
[i]Also at Università di Pisa, Pisa, Italy.
[j]Also at Università di Bari, Bari, Italy.
[k]Also at Sezione INFN di Trieste, Trieste, Italy.
[l]Also at Università degli Studi di Milano, Milano, Italy.
[m]Also at Universidade Federal do Triângulo Mineiro (UFTM), Uberaba-MG, Brazil.
[n]Also at AGH - University of Science and Technology, Faculty of Computer Science, Electronics and Telecommunications, Kraków, Poland.
[o]Also at Università di Padova, Padova, Italy.
[p]Also at Università di Cagliari, Cagliari, Italy.
[q]Also at MSU - Iligan Institute of Technology (MSU-IIT), Iligan, Philippines.
[r]Also at Escuela Agrícola Panamericana, San Antonio de Oriente, Honduras.
[s]Also at Scuola Normale Superiore, Pisa, Italy.
[t]Also at Hanoi University of Science, Hanoi, Vietnam.
[u]Also at P.N. Lebedev Physical Institute, Russian Academy of Science (LPI RAS), Moscow, Russia.
[v]Also at National Research University Higher School of Economics, Moscow, Russia.
[w]Also at Università di Roma Tor Vergata, Roma, Italy.
[x]Also at Università di Roma La Sapienza, Roma, Italy.
[y]Also at Università della Basilicata, Potenza, Italy.
[z]Also at Università di Urbino, Urbino, Italy.
[aa]Also at Physics and Micro Electronic College, Hunan University, Changsha City, China.
[bb]Also at School of Physics and Information Technology, Shaanxi Normal University (SNNU), Xi'an, China.